In Situ Exploration of Metallic Diaphragm Rupture in a Shock Tunnel

Yasseen Abdel-Magied*

Undergraduate Student, School of Mechanical and Mining Engineering, The University of Qld, 4067, Australia

Dr. David E. Gildfind†

Lecturer, School of Mechanical and Mining Engineering, The University of Qld, 4067, Australia

Douglas Malcolm‡

Workshop Manager, School of Mechanical and Mining Engineering, The University of Qld, 4067, Australia

Impulse facilities are an essential apparatus in the study of hypersonic flight. The experimental measurements taken from experiments conducted in these facilities are used in the study of flow behaviour and the verification and validation of predictive computational fluid dynamic or analytical models.

The impulse facility relies upon the rupture of a diaphragm separating gases in high pressure and low pressure tunnels to release the energy stored in the former as a brief hypersonic flow of gas.

In the impulse labs at the University of Queensland, the rupture of diaphragms occurs over a period on the order of 100 microseconds; sufficiently long to have an undesirable non uniform influence on the flow behaviour. In the analysis of experimental data, a constant rate iris opening model is used to model to account for the influence of the diaphragms boundary condition. This model introduces uncertainty into the predictive models as it does not account for the variability of opening rate, opening dynamics and tends to rely approximations of total opening time.

The purpose of this study is to improve the understanding and the ability to predict this boundary condition to facilitate the generation of more accurate models of impulse facility flows and in turn a higher degree of confidence in measured results used to quantify experimental results.

An experimental study was carried out on the three (3) metre long Drummond Shock Tube using 0.6mm thick, 5 series aluminium diaphragms. The rupture dynamics of scored, pierced and pressure burst diaphragms were filmed with three (3) high speed cameras and analysis of the data was conducted in Adobe Photoshop and Illustrator.

By comparing the results of the study to that observed in larger impulse facilities, a conceptual model which relates the resistance of the diaphragm to deformation may be related to the driving force from the facility to predict rupture behaviour. The next steps are to develop the pre-rupture finite element model (FEM) and to extend that to include simulations of diaphragm fracture with a vision to integrate this FEM into a Computational Fluid Dynamics (CFD) package where the dynamic deforming model may be used in the predictive models.

Nomenclature

$R.T$	Rupture Time
K	Experimental Rupture Coefficient
ρ	material density

*Mechanical and Aerospace Engineering Student ,The University of Queensland,St. Lucia, AIAA Student Member.

†Supervisor to Research Project,Centre for Hypersonics, The University of Queensland,Australia

‡Laboratory Technician,Department of Mechanical Engineering, The University of Queensland, Australia

τ	thickness
P_R	Pressure at Rupture
I	Inertia
θ	angle
M_1	Applied moment
M_2	Resistive moment
a	Crack branch half gap
b	Radial crack x distance from wall to branch
c	Radial crack y distance from wall to branch
A	Area Opened

I. Introduction

THE University of Queensland has invested extensively in it's hypersonic research program and notably, research into SCRAMjet technology and re-entry vehicles. Numerical computational methods are used to model and simulate what effect flight in supersonic and hypersonic regimes will have on a vehicle and conversely, what a vehicle must do to survive and perform optimally in such a regime. As is the case with all models, there is the need for verification through experimentation. In the field of hypersonic research in Australia, this means ground testing facilities are required and for flight conditions, impulse facilities are used.

Impulse facilities generate a brief, high speed flow that is directed over a model to simulate flow in hypersonic regime (Mach ≥ 5). There are several different types of impulse facilities, but each configuration is based around a basic shock tunnel whereby a test gas is processed with a moving shockwave generated through the release of energy in a driver gas. Yet due to the discrete nature of measurement devices, completely and reconstructing the behaviour in any Impulse facilities is not possible so CFD simulations and analytical models of facilities are used to predict and reconstruct.

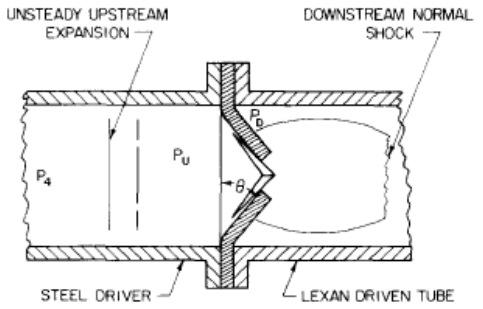

Figure 1. Barrel shock as represented by hickman [1] described as a simplification.

This report focuses on the behaviour of a single critical component found in Impulse facilities; the primary diaphragm. It influences shock formation distance, driver/driven gas mixing, vortices, acoustic noise and complex 3D shock structures as demonstrated by White , Campbell et. al, Simpson et. al, Hickman et. al and Gooze et. al .[3,4,5,1,6] These disturbance can also limit the operation of a facility by attenuating flow strength or vastly reducing flow uniformity [7] Diaphragm behaviours therefore must be simulated suitably to predict these flow characteristics in CFD models.

Current models of diaphragm opening used at the University of Queensland assume iris petal opening with timing based on the Rothkopf and Low model ,[8] essentially a generalised normalised curve of opening 2. The model introduces uncertainty in predictive models of impulse facility behaviour as deviation from the stated assumptions will compound error due to the generalisation of the model.

The aim of this study is to better quantify and understand the rupture of metallic diaphragms in impulse facilities to improve the predictive model. Eventually, this investigation is intended to improve this fundamental boundary condition in numerical and analytical models of impulse facility flow processes which may be used in designing new conditions or reconstructing test flows for unique tunnel and diaphragm configurations. This work will reduce one element of uncertainty. An experimental investigation of the behaviour of the primary diaphragm leading up to, and including, rupture was conducted in the Drummond reflected shock tunnel that was modified to operate as a shock tunnel. Measurement of scored, pierced and overpressure diaphragm rupture at various pressures has been conducted using high speed videography mounted externally to the tube and an optical/illumination system that allowed for the observation of rupture in situ.

II. Background

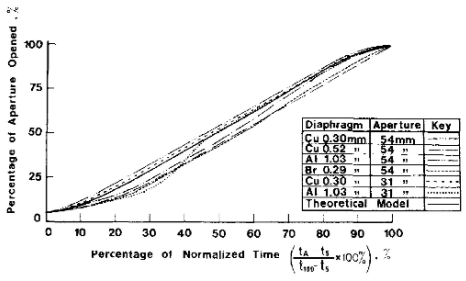

Figure 2. Rothkopf and Low standardised opening time of diaphragm compared with measured opening times. [2]

Impulse facilities may be described as "blast" (wind) tunnels used for studying the influence of high speed and high temperatures in hypersonic flight regimes .[9,10] A simplified description of the operation is that of an air cannon which is closest to a shock tube; the pressure in a reservoir (drive tube) is built up then released rapidly from the through a barrel (shock tube) positioned down stream. Rather than accelerate a projectile, the gas down stream (test gas) is accelerated by the driver gas and will flow through a test section between Mach 3 to 30 where hypersonic flow phenomena may be tested and studied .[11] The tunnels at the University of Queensland use diaphragm shock tubes whereby gas is compressed behind a diaphragm which acts as blowoff disc, releasing the highly compressed gas when it ruptures. The University of Queensland has four (4) impulse facilities. T4, a free piston reflected shock tunnel, X3 and X2, both free piston expansion tubes and Drummond, a reflected shock tunnel .[12] All have circular cross sections and are different lengths and diameters. The Drummond tunnel on which the experimentation is operated by pressurising a steel driver tube of fixed volume until the failure of the diaphragm. The X series and T4 tunnels use a free piston driver(s) that rapidly accelerates to 250 metres per second compressing and heating the driver gas .[11,10] The X2 uses a compound piston setup which experiences peak accelerations of up to 3500g and deceleration of up to 14000g depending on conditions .[8] These two methods of pre-rupture loading result in highly different loading conditions. The 3rd Volume of the Handbook on Shockwaves [7] provides information on the influence the configuation of the impulse facility downstream has on the gas.

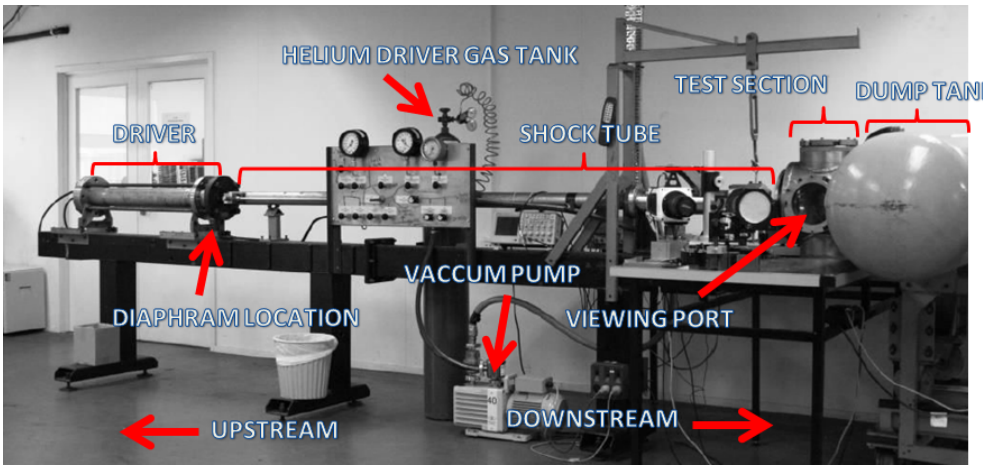

Figure 3. Image of the Drummond Tunnel

A. Drummond Tunnel

Drummond has 3 metre long shock tube with an internal diametre of 62 mm. The steel driver is one metre long and contains a pneumatic piercer. The diaphragm sits between the driver and shock tube and seals the ends of both tubes. Figure 3 shows the drummond tunnels configuration while figure 4 shows the diaphragm mounting surface on the driver and shock tube sides respectively. The reflected shock tunnel was modified to be a shock tunnel through the replacement of the reflection structure and nozzle with a straight section at the end of the shocktube. This was done to facilitate the experimental observation of rupture. As a result no seperation between the dumptank/test section and the shock tube existed in this setup. Ordinarily the former is maintained near vaccuum pressure so that start up is rapid and the energy of the flow can be dissipated. The latter is maintained at a pressure to represent the atmosphere of a planet.

B. Primary diaphragms

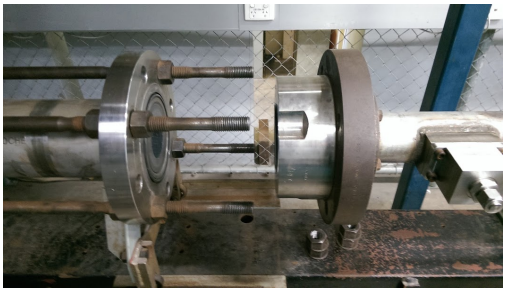

Figure 4. Driver mounting surfaces on Drummond Tunnel

When the pressure differential across a diaphragm is sufficient that the stress exceeds failure strength, the diaphragm will rupture. The greater the pressure differential between the pressure in the driver and shcok tube, the greater the shock speed [13] Prior to rupture, ductile metallic diaphragms deform and inflate forming hemispherical profiles.

On Drummond this pre-rupture process occurs on a time scale on the order of a minute while in piston driven facilities it can be between 10 milliseconds to 100 milliseconds depending on the size and configuration of the facility .[8] Figure 5 shows the pressure trace ahead of a diaphragm during the critical section of a piston stroke. The peak is indicative of the time of rupture while the brief spike ahead of this point represents the significant loading time.

On the downstream side of the diaphragm, lower pressure test gas fills the chamber. In ordinary operation, the test gas tube will be pumped down to between 16 kilo pascals and 35 kilo pascals The diaphragm responds to the pressure differential across it. Lower test gas pressures result in lower rupture pressures.

This following subsection details the models used to simulate the behaviour of diaphragms. This section is where the research presented in this project is conducted.

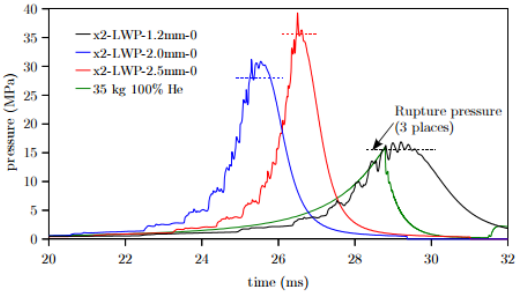

Figure 5. X2 diaphragm loading with the apex representing rupture time and the sharp increase representing significant loading time.

C. Diaphragm rupture analytical and approximate models

Over the past half century, multiple researchers have taken different approaches to characterise and model diaphragm rupture, opening time and interactions with the flow. The methods of rupture are overpressure or those initiated by defects such as scoreline or perforations from piercers or cuts from knife edges .[14] A generalised rupture time equation was developed (equation 1) and is based on equation (2) which relates the inertia of an opening diaphragm petal to the resistive moment. Different researchers took different approaches to arrive at rupture coefficients however an iris opening style is generally assumed (figure 6. In this profile, an initiating crack will form about the center of an inflated diaphragm and propagate outward in a cross pattern forming 4 petals which will accelerate under pressure loading and fold back along the test tube wall .[2]

$$R.T = K(\frac{L\rho\tau}{P_R})^{\frac{1}{2}} \tag{1}$$

$$I * \frac{d^2\theta}{dt} - M_1 - M_2 \tag{2}$$

Roshko (1961) [14] observed diaphragm opening time for various specific materials and conditions using a sharpened cross to initiate rupture. His research showed that very thin scribed diaphragms with thickness diameter ratios less that 0.1% may not fail along scribes. This introduces a degree of variation in overpressure rupture times and shapes. The Drummond tunnel diaphram is a 0.6 millimetre thick piece in a 62 millimetre tube has a ratio of 1%, suggesting that expected not to rupture along score lines is probable.

Campbell (1964) [4] used an optical photography technique to measure the opening time and generated a characteristic curve of the finite opening time for aluminium and copper diaphragms. Campbells research showed that the initial 20 % opening took around half the total opening time and that despite notching, the diaphragm burst unevenly.

Simpson (1967) [5] conducted an experimental investigation of a number of diaphragms of different materials while considering shock formation distance.The value for K is a function of angle of opening as in equation 3with K at an angle of 90 degrees equalling to 0.91 for an Iris diaphragm. Angle of opening is related to relative open area by equation 5. The thicker and more stiff the diaphragm is in bending, the less accurate this model is as it assumes a free hinged plate. If the opening is not the classical iris, whereby an initial vertical crack of half length a branches to form a triangle of height b and half length c producing two trapezoids and two triangles. In this case L from 1 becomes equation 4.

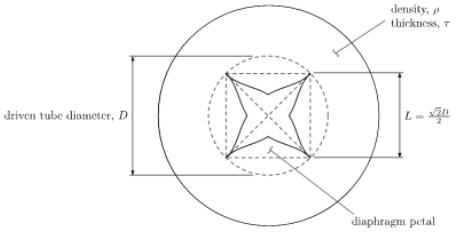

Figure 9.6: Schematic of rupturing diaphragm.

Figure 6. The petalling model is one model of the rupture of diaphragms that is used [8]

$$K = \int \frac{d\Theta}{[\frac{1}{2}sin2\Theta + \Theta]^{1/2}} \tag{3}$$

$$L = \frac{3ac + bc}{4a + 2b} \tag{4}$$

$$\frac{A*}{A} = 1 - cos(\theta) \tag{5}$$

Hickman et al. [1] modelled the resistive moment in equation 2 for thicker diaphragms as their bending stiffness and "strength coefficient" increases. The coefficient is a ratio of the resistive and applied moment. Thickness increases with the need to increase rupture pressure, and allow for scoring. While this is not particularly relevant to the thin aluminium diaphragms in Drummond which can be deformed by hand, it is relevant to the plain steel counterparts in the larger T4 facility at the University. This model assumes the petals are planar and does not consider membrane stiffness. This is relevant to thin ductile diaphragms such as the Drummond diaphragm which form (near) hemispherical structures prior to rupture and this induces a resistive moment.

Yamaki and Rooker [15] conducted experiments in 1972 and looked at the behaviour of grooved and knived plain steel diaphragms. They constructed a large dataset of K constants dependent on root thickness for use facilities with similar configurations. This variation is to be expected as the behaviour of failure will change if the rupture conditions (esp. strain rate) or material change.

Volkov et al. (1975) [16] modeled the diaphragm petals as"freely linked chain of masses" making the assumption that the driving forces were substantially greater than the material resistance. The K value calculated by back substituting the model into equation 1 was approimately 1.5 times less than the simpson value (0.6).The model is relevant when the diaphragm stiffness is low or the loading is very high. Zeitoun et al. [17] used both Simpson and Hickman models and found both accurate but the former easier to implement in simulations for a micro-shock tube. The 0.6mm aluminium diaphragm is elastic and must resist membrane stiffnes making this model inappropriate for this model

The Rothkopf and Low model [2] presents a linearly normalised opening aperture vs time trend to allow prediction of a functional dependence (figure 2). A constrant rate of opening between the first five(5)% and final opening is used with measured values for both times. Assuming that the aperture opening is crossed with four (4) petals 7 and dependent on the inertia of the petals. The model is suitable for predictive models in the absense of data such as that presented by Yamaki and Rooker as it sets out to characterise the behaviour rather than predict rupture rate accurately as may be observed by he overlayed diahragms of different materials in the figure.

A succinct list of k constants may be found in chapter nine of D. Gildfind .[8]

The Drummond Tunnel used with it's standard aluminium diaphragm of a 0.6mm thickness. Opening time constant will be taken from the simpson model and assumed to follow the normalised Rothkopf et al opening behaviour. This will serve as the basis for analysis in the discussion. The following section presents a brief discourse on the influence of the diphragm on Impulse facility behaviour adding more context to the motivation of this thesis.

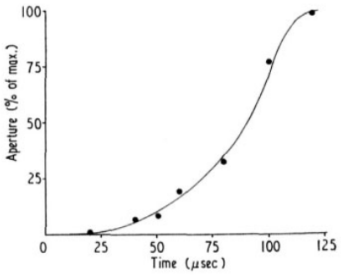

Figure 4. Variation of aperture size, observed photographically, with time for aluminium diaphragms.

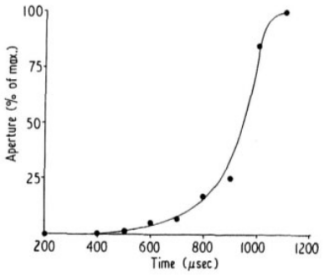

Figure 5. Variation of aperture size, observed photographically, with time for copper diaphragms. Driver diameter 3 in., driver pressure 145 lb in^{-2}.

Figure 7. Opening time with experimental points showing variance from model

III. Experimental Procedure

Pre rupture inflation was measured to allow for the detemination of material properties. This was achieved by pressurising the driver with the diaphragm inserted and removing it at a certain pressure then measuring the deflection. From the deflection, the effective radius is calculated assuming a hemispherical profile. This arc length may then be calculated and the ratio of this to the original diametre is used to determine the geometric strain. On a thin diaphragm such as this, the thin walled pressure vessel equation is assumed to be reasonable and this allows for an estimation of the stress from the pressure, thicknss and radius. Finally, the stress may be graphed againsts the strain to give a modulus profile which may be used as the material behaviour in a simulation.

The rupture of the diaphragm was observed within the shock tube. A mirror mounted inline with the shocktube on a sting in the test section that would otherwise hold models was offest by an angle of 45 degrees allowing for the illumination of the diaphragm as well as the observation. Illumination was achieved through the collumation of a 2450 Lumen green led illuminator and the direction of this light onto a diaphragm. The diaphragm would be painted white so it had a diffuse surface which reflects light of the hemispherical pre-ruptured diaphragm more effectively. The aluminium diaphragm is far to reflective and will only effectively reflect light from the tip, limiting the observable area. A high speed cameras was then directed at the 45 degree mirror with a 70-200mm lens to focus on the 62mm diaphragm 4 meters away and observe rupture. Triggering of the camera recording stopped a continuous loop after a short delay. The triggering mechanism was the amplified signal of a PCB pressure transduceras it responed to the shockwave in the shock tube. The transducer positioned less than 200mm away from the diaphragm loaction triggered while the diaphragm was still rupturing requiring a delay on timing. Figure 7 shows this figure.Following rupture, adobe photoshop was used to enhance the imae and illustrator was used to trace the rupture profile and determine the rupture opening angle

IV. Results

A. Pre-rupture Deformation Results

Some of the diaphragms obtained through the pre rupture process described in the implementation section can be observed in figure 9. Six (6) diaphragms were generated at pressures as listed in table 1. Their height was measured using a tabletop caliper.

Using the technique outlined in the background, the geometric circumferential strain was calculated. Figure 10 is a plot of the strains and the deflections with a line of fit. Then assuming a spherical pressure vessel, the stress strain graph can be produced as in figure 10.

figure 14 on page 11.

The stress strain curve can be improved and bolstered with more data for use as modulus data in the computational FEA simulations while the original deflections serve as the verification.

B. Ruptured Results

This subsection looks at the behaviour of the diaphragm rupture in three conditions; those are:

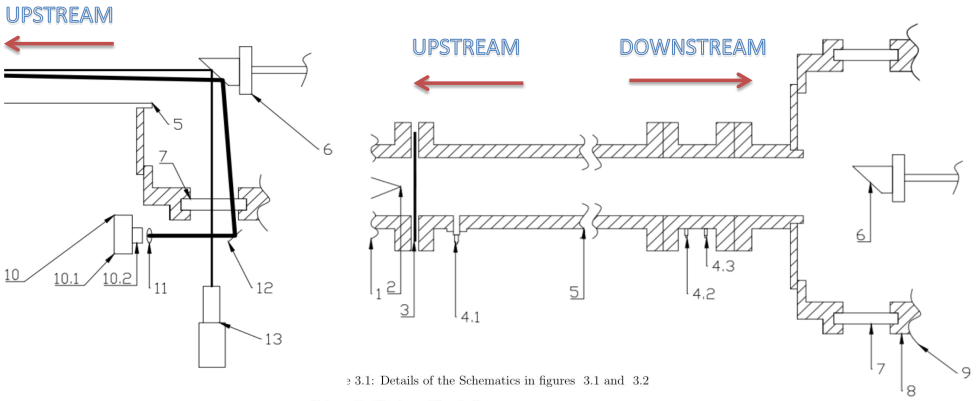

› 3.1: Details of the Schematics in figures 3.1 and 3.2

Schematic Number	Description
1	High Pressure Resevoir
2	Piercer
3	Diaphragm
4a	Triggering Pressure Transducer
4b	Pressure Transducer
4c	Temperature Gauge
5	Test Gas Shock Tube
6	45 Degree Flat Mirror Mounted on Sting
7	Test Section Window
8	Test Section
9	Dump Tank
10	LED
10a	Heat Sink
10b	Reflective Tube
11	Focussing Lens
12	Flat Mirror
13	High Speed Camera

Figure 8. Optical and Sensor Setup on Drummond

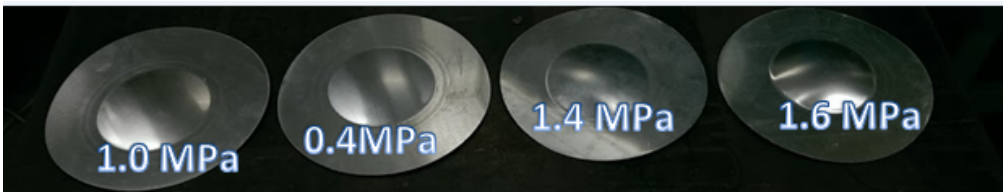

Figure 9. Inflated Diaphragms. Note the spherical shape

- Overpressure Rupture
- Pierced Rupture
- Scored Overpressure Rupture

Piercing was conducted at a number of pressures with a pneumatic piercer. The damage profile the piercer induces on the diaphragm can be seen in figure 12 where a diaphragm vented rather than ruptured following piercing at 1.5 megapascal. figure 11 on the next page.

Figure 12. The influence of the piercer on the diaphragm.

The piercer was used to rupture the diaphragms at a range of pressures and allowed for the observation of rupture behaviour in different pressure ranges. The raw figure and processed figure in 11 shows the rupture behaviour following piercing. In the first image, note the "double door" profile where the crack propogated to the wall and branched near it. The same behaviour can be seen is diaphragm t2. In the second image, the main petals formed are closer to squares than triangles. Between larger petals sit smaller petals. The rupture originated from a single crack that branched, explaining the shape of the ruptured part. The root of the petals are almost square except for the larger petals, which have localised buckling (visible in top right petal)

Overpressure is achieved by gradually increasing the pressure in the driver tube until the unassisted rupture of the diaphragm is achieved. This occurred when the pressure difference

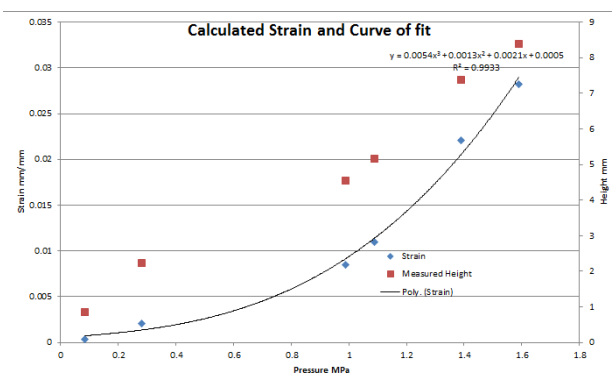

(a) strain and deflection graph

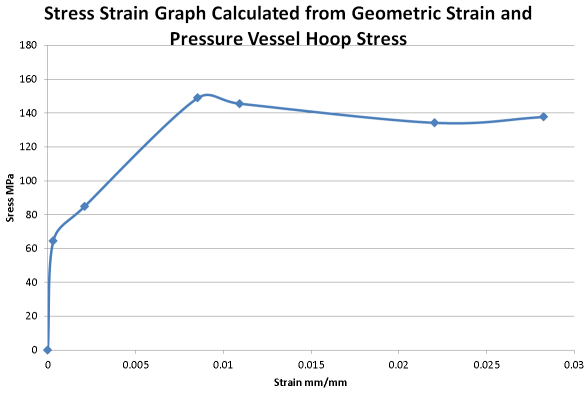

(b) stress strain graph

Figure 10. Pre rupture graphs.

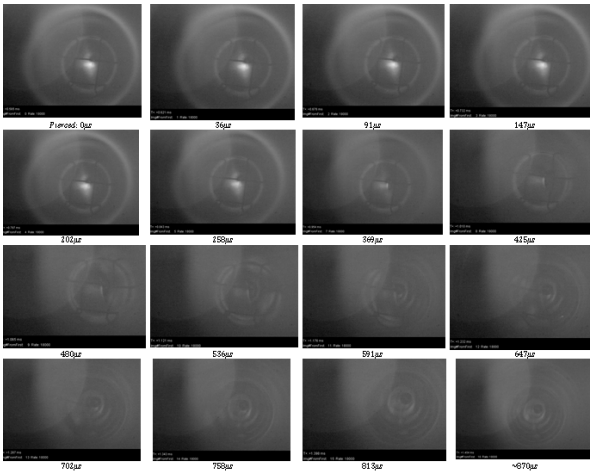

(a) Raw images from High Speed camera

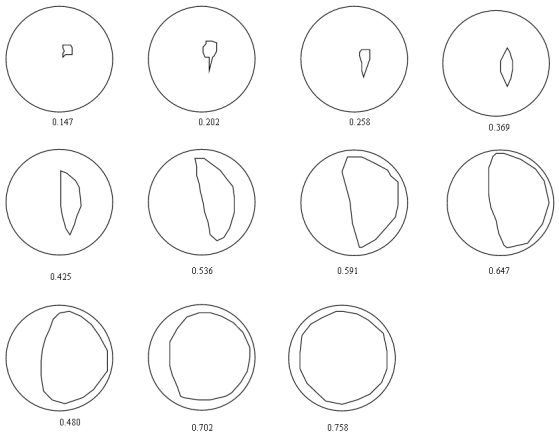

(b) Processed images from which the area ratio may be calculated

Figure 11. Diaphragm Rupture Captured with Phantom at 18000FPS

Table 1. Pressures of the Inflated Diaphragms

Inflation Pressure difference MPa	Deflection in mm
0.09	0.86
0.29	2.24
0.99	4.55
1.09	5.16
1.39	7.38
1.49	8.39
2.85+	Ruptured

across the diaphragm was between 2.85 to 3.25 megapascals. Ruptures are initiated about the centre when the in plane stress is greater than the failure stress. Due to material variability, this leads to slight differences in the inital poisition of diaphragms ruptured as well as load. For example, in one case a hairline crack appears on the diaphragm for several hundred frames, an order of magnitude longer than the rupture process, while in other cases it took less than 30

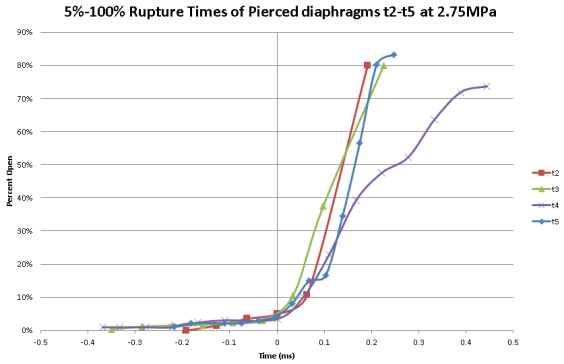

Figure 13. Graph of the opened area of pierced diaphragms ruptured at 2.75MPa shown in and biased by 5% to agree with the rothkopf model.

This may be the result of the filling rate fluctuating, however the pierced diaphragms ruptured when the filling rate was zero indicating that the formed crack was sufficiently small to somehow remain stable. However the resultant profiles remained quite consistent. The irregular initial rupture patterns are similar as to those as shown in .[18] The difference is that the petalling does not produce triangular shapes. The overpressure diaphragms petals of the opening sections opened completely flattened themselves against the shock tube wall. Figure 14 shows the raw rupture images taken of one shot and the processed outlines of overpressure ruptured diaphragms.

A comparison of two overpressure ruptures is shown in figure 16 were there is a clear difference in behaviour and trend. The difference was in how the cracks propogated. One branched as in 10 while the other had a singular petal fold to the wall before noticable rupture extended to the rest of the diaphragm. .The implication is that this may make it very difficult to predict rupture. Overpressure has a more uniform end shape but was suseptable to high variation in time of opening due to unassisted crack initiation uniform than pierced.

Scoring of the diaphragm produced reliably consistent trapdoor opening diaphragms. The diaphragms all ruptured below 1.5 megapascal, below the minimum rupture point for an unscored diaphragm. Higher dimensional consistency in creating the scores may have achieved petalling as opposed to trap door opening. The opening time of the diaphragm was not explored however a quantitative analysis may be found in the following section.

V. Discussion

It is known from research that different diaphragms will act differently. The results showed a few things. When rupture is not forced or artificially induced, it may follow a general trapdoor or petalling behaviour however material properties relevant to fracture and the loading conditions will influence behaviour. A qualitative explanation of the shape of rupture that is formed may be adapted from an energy methods analysis of fracture mechanics. The driving force is dependent on the rate and level of loading of the driver gas as well as the area interacting with the flow. The resistance to folding is dependent on stiffness of the material and the dimensions / structure at the root. Assuming that rupture starts from a single crack at the centre of an inflated diaphragm:

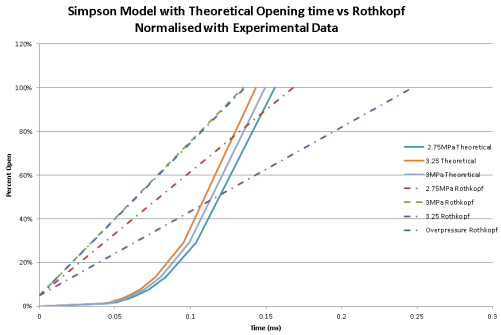

Figure 15. Opened area of the diaphragm modelled with the rothkopf model with the original simpson model for opening in place

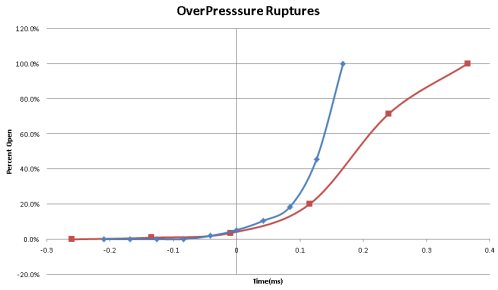

Figure 16. Opened area overpressure rupture diaphragms

- trapdoor opening will occur as there is not enough energy to encourage complete removal of material from the flow
- A high driving force relative to resistance will demand removal from the flow path. As the crack initally propogates, it is effectively a large petal and due to the dimensions and shape is highly resistant to folding to the wall of the shock tube is high.
  - The petal can reduce in size by
    - branches the crack to form rectangular and triangular peta
    - The crack surfaces serve as the initiation point of new cracks resulting in more petals
  - Even with more petals, high curvature at the base can introduce more strain. Relief is achieved by any of or a acombination of the following:
    - Buckling about the root
    - Circumferential tearing
    - Formation of small petals near the base

The diaphragm will rupture in the manner which relieves the pressure effectively while requiring the lowest energy. For example, scored diaphragms offer a path of low resistance. Thin diaphragms such as the Drummond diaphragms are more likely to buckle than thicker stronger equivalents such as the X2 equivalents which will tear circumferentially. The formation of new crack surfaces is highly energy consuming so will likely occur with high loads applied.

This qualitative description of opening ties in appropriately with the opening time for the diaphragms. It was found that what we have is quite accurate but precision is low as the behaviour of diaphragms would differ. With artifical stress raisers more predictability is achieved in the opening rate and dynamics. Thus acoustics can be better accounted for and are more likely undesirable perturbations will be more predictable. More predictability will enable more accurate models to be developed.

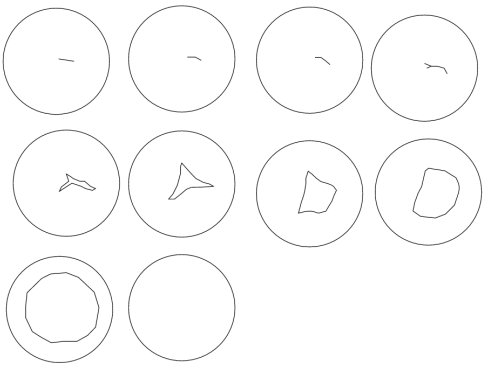

Figure 14. Diaphragm Rupture Captured with Phantom at 24000 FPS at overpressure at 3.25MPA w/ 30KPa Back Pressure.

Future research should look at different scoring patterns and to adapt chemical engineering burst discs to the shocktube namely the selection of number of petals and the use of alternative scoring outlines.

VI. Conclusion

The University of Queensland's predictive models of impulse facilities use a simplified diaphragm opening model as a boundary condition. This model assumes a constant opening rate and an iris opening profile designed for use in the absence of more precise data. This thesis endeavored to quantify and better understand the diaphragm rupture process in an effort to take the first steps in reducing uncertainty introduced by an approximate model.

To achieve this goal, experiments were conducted where the rupture of diaphragms was measured using a high speed camera in the Drummond shock tunnel. Scored, pierced and overpressure ruptured Aluminium diaphragms at pressure differentials of 1.4 mega pascals, 2.75 to 3.25 megapascal and greater than 3.25 megapascal respectively was observed.

The observations carried out were on low pressure and strain rate loading conditions relative to larger facilities ruptured at the University of Queensland. This allowed for the observation of the behavior change from trap door at low pressures to iris opening at high. Only scored diaphragms were consistent in their behaviour as a path for the initiation of the crack is provided. Pierced diaphragm rupturing at the same pressure would present composite ruptures of trapdoor and iris opening diaphragms, i.e double door opening. This behaviour of the diaphragm petals or door after initiation is related to the diaphragm's resistance to removal as a flow obstruction indluding its inertia and resitive moment and the load applied by the flow on the diaphragm A stiffer diaphragm resists this force more intensely where stiffness is dependent on shape, thickness and material properties. The dynamics of opening of is influenced by the governed by the drive to relieve the stress as effectively as possible with the least expenditure of energy.

When a diaphragm ruptures initially, a single crack will appear at the center of the diaphragm. If there is iris scoring present and the driving force is sufficient, the cracks will propagate along the scores. Otherwise a crack may branch or form new cracks on the crack face creating petals. Creating crack faces expends energy and so the load must be high relative to material resistance for new surfaces to form. As the crack reaches the walls of the diaphragm, its root curvature will give it an amount of membrane stiffness and the larger the petal, the more stiffness it will have. To relieve the pressure, the root will fold to the wall, tear along its boundaries reducing the membrane stiffness resistance or buckle and crumple to fold to the wall. If the load is low, incomplete rupture can occur as the created hole provides sufficient pressure relief for the driver gas.

Despite this general rupture process, there was still variation in how the unique diaphragm behaved leading to variation in opening time Thus for the aim of reducing uncertainty using scored diaphragms is the recommendation. Investigation of sealed slotted diaphragms such as those used in chemical engineering applications is also recommended as it provides an opportunity to even lower resistance diaphragms while maintaining rupture pressure for a given thickness

References

[1]Hickman, R. S., Farrar, L. C., and Kyser, J. B., "Behavior of burst diaphragms in shock tubes," *Physics of Fluids (1958-1988)*, Vol. 18, No. 10, 1975, pp. 1249–1252.

[2]Rothkopf, E. and Low, W., "Diaphragm opening process in shock tubes," *Physics of Fluids (1958-1988)*, Vol. 17, No. 6, 1974, pp. 1169–1173.

[3]White, D. R., "Influence of diaphragm opening time on shock-tube flows," *Journal of Fluid Mechanics*, Vol. 4, No. 6, 1958, pp. 585–599.

[4]Campbell, G., Kimber, G., and Napier, D., "Bursting of diaphragms as related to the operation of shock tubes," *Journal of Scientific Instruments*, Vol. 42, No. 6, 1965, pp. 381.

[5]Simpson, C., Chandler, T., and Bridgman, K., "Effect on shock trajectory of the opening time of diaphragms in a shock tube," *Physics of Fluids (1958-1988)*, Vol. 10, No. 9, 1967, pp. 1894–1896.

[6]Goozée, R. J., Jacobs, P. A., and Buttsworth, D. R., "Simulation of a complete reflected shock tunnel showing a vortex mechanism for flow contamination," *Shock waves*, Vol. 15, No. 3-4, 2006, pp. 165–176.

[7]Ben-Dor, G., Igra, O., and Elperin, T., *Handbook of Shock Waves, Three Volume Set*, Elsevier Science, 2000.

[8]Gildfind, D. E., *Development of high total pressure scramjet flow conditions using the X2 expansion tube*, Ph.D. thesis, University of Queensland School of Mechanical and Mining Engineering, 2012.

[9]Burn, R., "Shock Tubes and Shock Tunnels: Design and Experiments," sep 2009.

[10]Gildfind, D. E., "Part 2: Hyper-sonic Ground Testing, Local surface inclination techniques and Viscous Hyper-sonic Flow," Lecture Slides From MECH447.

[11]Stalker, R. J., "Modern developments in hypersonic wind tunnels," *Aeronautical journal*, Vol. 110, No. 1103, 2006, pp. 21–40.

[12]of QLD, T. U., "Impulse Facilities," 2015.

[13]Anderson, J., *Modern Compressible Flow: With Historical Perspective*, Aeronautical and Aerospace Engineering Series, McGraw-Hill Education, 2003.

[14]Roshko, A. and Baganoff, D., "A novel device for bursting shock-tube diaphragms," *Physics of Fluids*, Vol. 4, No. 11, 1961, pp. 1445–1446.

[15]Yamaki, Y., Rooker, J., Center, L. R., AERONAUTICS, N., and CENTER., S. A. L. S. V. L. R., *Experimental Investigation of Circular, Flat, Grooved and Plain Steel Diaphragms Bursting Into a 30.5-centimeter-square Section*, NASA technical memorandum, Defense Technical Information Center, 1972.

[16]Volkov, V., Parmon, V., and Tkachenko, B., "Process of opening of an inelastic diaphragm in a shock tube," *Journal of Applied Mechanics and Technical Physics*, Vol. 18, No. 4, 1977, pp. 506–509.

[17]Zeitoun, D. E. and Burtschell, Y., "NavierStokes Computations in Micro Shock Tubes," *Shock Waves*, Vol. 15, No. 3, 2006, pp. 241–246.

[18]Gaetani, P., Guardone, A., and Persico, G., "Shock tube flows past partially opened diaphragms," *Journal of Fluid Mechanics*, Vol. 602, 2008, pp. 267–286.